



BNL-212466-2019-JAAM

Using In Situ and Operando Methods to Characterize Phase Changes in Charged Lithium Nickel Cobalt Aluminum Oxide Cathode Materials

S. Hwang,

To be published in "Journal of Physics D: Applied Physics"

December 2019

Center for Functional Nanomaterials
Brookhaven National Laboratory

U.S. Department of Energy
USDOE Office of Science (SC), Basic Energy Sciences (BES) (SC-22)

Notice: This manuscript has been authored by employees of Brookhaven Science Associates, LLC under Contract No. DE-SC0012704 with the U.S. Department of Energy. The publisher by accepting the manuscript for publication acknowledges that the United States Government retains a non-exclusive, paid-up, irrevocable, world-wide license to publish or reproduce the published form of this manuscript, or allow others to do so, for United States Government purposes.

DISCLAIMER

This report was prepared as an account of work sponsored by an agency of the United States Government. Neither the United States Government nor any agency thereof, nor any of their employees, nor any of their contractors, subcontractors, or their employees, makes any warranty, express or implied, or assumes any legal liability or responsibility for the accuracy, completeness, or any third party's use or the results of such use of any information, apparatus, product, or process disclosed, or represents that its use would not infringe privately owned rights. Reference herein to any specific commercial product, process, or service by trade name, trademark, manufacturer, or otherwise, does not necessarily constitute or imply its endorsement, recommendation, or favoring by the United States Government or any agency thereof or its contractors or subcontractors. The views and opinions of authors expressed herein do not necessarily state or reflect those of the United States Government or any agency thereof.

**Using *In Situ* and Operando Methods to Characterize Phase Changes in Charged Lithium
Nickel Cobalt Aluminum Oxide Cathode Materials**

Sooyeon Hwang^{1*}, Eric A. Stach^{2*}

¹Center for Functional Nanomaterials, Brookhaven National Laboratory, Upton, New York 11973,
United States

²Department of Materials Science and Engineering, University of Pennsylvania, Philadelphia,
Pennsylvania 19104, United States

*Corresponding Authors: soohwang@bnl.gov; stach@seas.upenn.edu

Abstract

Lithium ion batteries have been extensively explored in recent decades in order to improve their electrochemical performance, address safety concerns, and reduce costs in larger-scale applications. Electrode materials are key components which govern the properties of the battery at the system level. Cathode materials are of particular importance as they are a limiting factor for achieving high energy density. Lithium nickel cobalt aluminum oxide ($\text{LiNi}_{0.8}\text{Co}_{0.15}\text{Al}_{0.05}\text{O}_2$, referred to subsequently as NCA) is one of successful cathode materials since it can deliver higher capacity than other cathode materials such as lithium cobalt oxide or lithium iron phosphate. However, structural instabilities that occur NCA during charging or at high temperatures is believed to be the primary reason for performance degradation as well as a possible safety threat. Thus, understanding the structural evolution that occurs in NCA is of importance to acquire fundamental insights for taking full advantage of the high capacity of NCA materials. Beyond static information, *in situ* and *operando* characterization approaches allow us to observe structural changes under external stimulus or in a working condition, providing a deeper understanding of the routes by which structure evolve. In this review, we will describe the use of both *in situ* and *operando* characterization performed with both synchrotron X-ray based techniques and advanced electron microscopy, as the combination of these techniques have been shown to be particularly effective at providing structural information at complementary length scales.

1. Introduction

Lithium ion batteries (LIBs) have been critical to powering electronic devices since their first commercialization in 1991, and the importance of this technology has been recognized through the awarding of the 2019 Nobel Prize in Chemistry to John Goodenough, Stan Whittingham and Akira Yoshino for their development of this technology [1]. The initial LIB was commercialized with non-graphitizable carbon as the anode and lithium cobalt oxide (LiCoO_2) as the cathode material[2]. LiCoO_2 has the $\alpha\text{-NaFeO}_2$ layered structure, where oxygen has a cubic close packed arrangement and Li and Co occupy octahedral sites alternatively as shown at Figure 1a. Li can electrochemically be extracted and inserted from/into LiCoO_2 at around 4 V vs Li^+/Li ; thus, it can serve as an effective cathode material in LIBs. The reversible capacity is relatively low at around 140 mAhg^{-1} because only half of lithium can be reversibly cycled without capacity loss [3]. When more than 0.5 Li is extracted, oxygen starts participating in the redox reaction by forming peroxides, which may lead to oxygen loss and eventually, decomposition of the compound [4]. In addition, there is a limited availability of Co, and as a result, various combinations of transition metals (TMs) has been attempted to replace Co as well as to improve the overall electrochemical properties of the materials. Ni-rich LiTMO_2 have been proposed as successful alternatives to LiCoO_2 [5-10] and $\text{LiNi}_{0.8}\text{Co}_{0.15}\text{Al}_{0.05}\text{O}_2$ (NCA) is one of the most successful composition as cathode materials. The Ni-rich composition provides a high capacity while Co and Al substitution increases structural stability [11,12].The virtue of NCA as a cathode material is its high capacity and power density [12,13], which makes NCA an attractive cathode material even in larger-scale applications, particularly battery-operated electric vehicles (BEVs). Currently, Tesla uses NCA chemistry for its EVs. The LIB cells used in the Tesla model 3, composed of NCA (cathode) and Si/C or SiO_x/C (anode), deliver specific energy of 260 Wh kg^{-1} and energy density of 683 Wh l^{-1}

at nominal voltage of 3.6 V in cell, outstanding performance when compared to other commercial EVs [14]. However, there is a strong desire for even greater energy densities. The US Department of Energy and the Advanced Battery Consortium have suggested at least a 500 km driving range per single charge is required in order to achieve mass market penetration of BEVs, which corresponds 350 Wh kg⁻¹ and 750 Wh⁻¹ at the cell level [14]. To meet these requirements, cathode materials need to deliver at least 202 mAh g⁻¹ at 3.7 V [13].

When considering the high capacity of NCA (~200 mAh/g), the choice of NCA as the cathode material for BEVs application thus appears reasonable. However, NCA still has room for development. The high energy density of NCA achieved in the cycles is a desirable but significant capacity loss of NCA has been reported during long-term cycling [15-17]. The layered structure of NCA can be destroyed as a result of repetitive lithium movements or *via* exposure to high temperatures, resulting in phase transformations from the α -NaFeO₂ layered structure (space group: $R\bar{3}m$) to spinel ($Fd\bar{3}m$) and rocksalt ($Fm\bar{3}m$) (Figure 1). These structures have similar oxygen frameworks, and thus the phase transformations take place as a result of cation mixing. Phase transformations of layered cathode materials have been ascribed as the root cause of performance degradation, such as capacity fading and impedance rise [18-24]. Furthermore, issue concerning safety is another significant hurdle for the widespread application of NCA. Phase transformations are accompanied by oxygen gas evolution, which can react with the flammable electrolyte inside LIB cells. In the worst case, catastrophic explosions may happen. In other words, the structural instability NCA has a detrimental effect on both capacity fade and overall safety. Thus, diagnostic analysis has been performed by investigating NCA materials after they have been subject to electrochemical tests, providing valuable insights in the correlation between structural changes and performance degradation [25-30]. However, limitations of post-mortem studies still remain:

physical and (electro)chemical properties of NCA cathode materials can be altered after being removed from their working environment. For example, even though it is possible to acquire electrode samples right after reaching certain states of charge (SOCs) or cut-off voltages, it is uncertain that the electrode material being investigated represents the SOCs or voltages present at the SOC [31]. Electrodes are generally cleaned with dimethyl carbonate (DMC) solutions, one of solutions in conventional electrolytes, and this process may also change the surface chemistry [31,32]. For electron microscopy studies, focused ion beam (FIB) method can be used for thinning the sample, but this too can bring about unwanted physical damage to the samples. Furthermore, it is impossible to track the dynamics of structural evolution using standard TEM approaches.

To overcome these issues, *in situ* and *operando* methods have been utilized. “*In situ*” is a Latin phrase, meaning ‘in the original place’. *In situ* analysis refers to the real-time analysis of the sample under the application of external stimulus (for example, mechanical, electrical, magnetic, temperature, environment, *etc.*) at the same place. *Operando* studies are a combination of *in situ* analysis and performance measurement, which can provide a direct link between the structure and properties of materials while they are performing their function (i.e. ‘in a working condition’ – the Latin translation of *operando*). Exploring a material while it is in a working state enables researchers to circumvent undesirable aspects of ex-situ studies. As a result, various *in situ* and *operando* methods have been exploited to elucidate charge mechanisms or degradation mechanisms of NCA cathode materials. In this review, common *in situ* and *operando* analysis methods used for NCA studies based on X-ray based techniques and transmission electron microscopes are introduced and representative *in situ* and *operando* studies regarding NCA cathode materials will be discussed. This review will show *in situ/operando* analysis have

advanced our understanding of NCA cathode materials with respect to two specific topics: i) structural and chemical evolutions that occur during electrochemical reactions and their link with degradation mechanisms of NCA materials and ii) thermal stability at high temperatures to address safety concerns in NCA materials.

2. *In situ* and *operando* characterization tools for NCA materials

2.1. Synchrotron X-ray based techniques

Compared to laboratory X-ray sources, synchrotron X-ray can provide significantly better spatial and temporal resolution [33], which allows examination of both subtle and instantaneous changes occurring in the specimen, making synchrotron X-ray based techniques powerful tools for *in situ/operando* studies. X-ray scattering, which includes X-ray diffraction (XRD) [33-36] and pair distribution function (PDF) [37-39], and x-ray absorption spectroscopy (XAS) [40-44] have been applied to track the changes in crystal structure and chemistry of electrode materials, respectively. XRD is a powerful method for studying the crystal structure of materials. PDF, also known as total scattering, is particularly beneficial to studying short-range order in the structure. XAS includes X-ray absorption near edge structure (XANES) and extended X-ray absorption fine structure (EXAFS), and is classified according to the energy range from which the analysis is made. XANES (± 50 eV relative to the absorption edge) is beneficial to probe the chemical information, e.g. oxidation states and coordination symmetry of the excited element. From EXAFS (40 to 1500 eV beyond the absorption edge), we can acquire structural information, e.g. coordination number and bond distance [45]. With appropriate beamline design, imaging a sample is also feasible. Transmission X-ray microscopy (TXM) requires the brightness and coherence of 3rd generation synchrotron X-ray sources, and allows reconstruction of the 3-dimensional structure of the sample

at nanoscale resolution [33,46-48]. Furthermore, TXM can be integrated with other techniques like XAS (in full-field TXM), and is thus beneficial for providing a comprehensive understanding of chemical properties, elemental distributions, and the morphology of samples [33,49-51].

Real-time X-ray analysis can be realized through proper sample preparation. Figure 2a, b presents schematics of a modified coin cell (Fig 2a) and pouch cell (Fig 2b) for *in situ/operando* X-ray analysis. For X-ray penetration, both the coin cell and pouch cell configuration are modified with coaxial holes. The holes are generally covered by polyimide tape to confine the liquid electrolyte due to its high transmittance to X-rays. Beyond this simple modification of pre-existing cells, various types of *in situ* cells have been carefully designed for characterizing LIBs with X-ray based techniques, for example, Argonne's multipurpose *in situ* X-ray (AMPIX) electrochemical cell [52], soft XAS cells [53], capillary type cells [54], and microfluidic electrochemical cells [55].

In the case of NCA materials, thermal stability is one of key factor governing battery safety; thus, structural and chemical evolution at high temperatures have also carefully examined. Figure 2c shows an experimental setup that combines time-resolved, temperature dependent XRD and mass spectroscopy, which permits detection of changes in crystallographic structure and correlated release gaseous species from a sample simultaneously [56].

2.2. Transmission electron microscopy

Transmission electron microscopy (TEM) can offer exceptional imaging performance (sub-Angstrom spatial resolution) as well as diffraction and spectroscopy; thus, it has been actively utilized in battery society to identify the morphology, crystal structure, and chemical information of electrode materials at nanoscale before and after electrochemical tests [22,57-62]. It generally operates either with a parallel electron beam (TEM mode) or a focused, small probe scanning over the sample (scanning TEM, STEM mode). High-resolution TEM images (HRTEM) in TEM mode

are formed by interference between transmitted and diffracted electron beams (phase contrast), but because of complications associated with lens aberrations and sample thickness effects, the interpretation of HRTEM images is not straightforward. In contrast, the image contrast at STEM mode is approximately proportional to Z^2 (Z: atomic number) with a high-angle annular dark-field (HAADF) detector. This simple scaling of image intensity with atomic number allows more straightforward image interpretation: the strong contrast of TM layers in the layered structure can be easily defined, although the visualization of Li is not possible with this approach. Thanks to Z-constant of HAADF-STEM, cation mixing can be visualized at the atomic level. The combination of STEM and energy dispersive X-ray spectroscopy (EDX) or electron energy loss spectroscopy (EELS) enables chemical information at nanoscale, such as elemental distribution and oxidation state of TMs [41,63-65]. Therefore, HAADF-STEM imaging and STEM-EELS/EDX have become a routine technique for the studying layered structure of cathode materials [24,66-69].

Along with the multifunctionality at high spatial resolution, one of the biggest benefits from TEM is its '*in situ*' capability. It is possible to acquire images, diffraction patterns and EELS/ EDX spectra under various external stimuli (gas/liquid environment, biasing, temperature, *etc.*), which can be applied by using a specialized sample holder. In order to explore electrode materials for LIBs, *in situ/ operando* TEM is becoming a popular approach. Dry-format electrochemical cell (Figure 2d) was realized for investigating phase evolutions occurring at electrode materials during *in situ* lithation/ delithiation [70-73]. In this configuration, Li metal is used as the anode and an ionic liquid or naturally oxidized Li_2O layer serves as the electrolyte. Despite fruitful insights on structural changes of materials with Li, the dry-cell setup has a clear limitation. As real LIBs are composed of liquid electrolytes, the structural evolutions that occur using the dry-cell approach may not accurately reflect the real case [74]. Using the liquid-cell, one can build an electrochemical

device inside microscope that is more relevant to real LIBs [75-77]. Figure 2e presents a cross-sectional view of the liquid-cell experimental setup. Liquid electrolyte is separated from high vacuum of microscope by being confined with nitride windows and electrodes are incorporated in microfabricated Si chips for biasing. Electrochemical reactions have been observed *in situ/operando* at various anode materials; however, relatively few studies have been published on cathode materials [72,75,78,79] and to our best knowledge, lithium extraction/insertion from/into NCA has not been observed *in situ/operando* inside TEM.

Instead, the thermal stability of NCA has been carefully examined at nanoscale *in situ*. The temperature of the sample can be increased by using two kinds of heating holder (Figure 2f) [80]: a furnace-type heating holder that is designed to use standard TEM grids, or a microfabricated heater that is specially to heat a localized area through Joule heating of a thin film. The furnace-type of holder has an advantage in that sample preparation is much easier, but the microfabricated holders can control temperature more precisely with minimized sample drift.

3. *In situ/Operando* studies for elucidating charge/degradation mechanisms of NCA

NCA cathode materials mediate electrochemical reactions *via* intercalation, where Li ions are extracted from / reinserted into the original structure with minimum structural change. To elucidate the subtle structural changes occurring in NCA, synchrotron-based *in situ* XRD has been used. Yoon *et al.* [81] demonstrated that three hexagonal phases (H1, H2, H3) are associated with NCA during the initial charge to 5.2 V. A new hexagonal phase evolves at the expense of a pre-existing phase, suggesting a two-phase reaction mechanism. In addition, it was suggested that the lattice parameter along *c*-axis expands with contraction of that along *a* and *b* axes in early stages of charging, but thereafter the *c* lattice parameter shrinks along with a slight expansion of the *a* and

b lattice constants at high voltages. Robert *et al.* [82] presented *in situ* XRD patterns of NCA acquired during the first 3 cycles between 3.0-4.9 V, indicating that reaction mechanism of the first cycle is different from the second and following cycles. Figure 3a presents changes in 003 reflection of NCA during the first and second charge. While the first charge takes along with a two-phase transition and solid solution mechanisms, the second charge is dominated by a solid solution mechanism, reflected in a continuous change in position of the diffraction peak. On the other hand, Grenier *et al.* [83] suggested that the ‘two-phase’ behavior is primarily a result of the reaction inhomogeneity between secondary NCA particles induced by nonuniform erosion of the Li_2CO_3 surface layer. In this case, comparisons between the reaction behavior of NCA with and without the Li_2CO_3 layer, were made by obtaining *in situ* XRD patterns acquired during the first cycle (4.1-2.7 V) from two kinds of NCA materials, which were stored under ambient condition and inside of argon-filled glove box, respectively.

Overcharging of LIBs can lead to a serious safety threat because of heat generation from unwanted chemical reactions between the delithiated cathode or lithiated anode and the electrolyte [84,85]. Local accumulation of heat may lead to catastrophic failure as a result of thermal runaway. Thus, investigating the structural and chemical evolution of electrode materials when they are exposed to harsh operating conditions is important to guarantee safe operation of LIBs. Lin *et al.* [86] took advantage of *in situ* high-energy XRD to identify the failure mechanism of 18650-size LIB. Local temperatures of both the cathode (NCA) and the anode (graphite) sides were estimated using lattice expansion of Al and Cu, which are the current collector for cathode and anode, respectively. During charging, a temperature increase was noticed at cathode side around 4.16 V and the temperature kept increasing with further charging. In contrast, temperature increases in the anode side initiated at much higher voltage of 4.58 V. Makimura *et al.* [87] investigated side reactions

occurring at the positive NCA and negative graphite electrodes using *in situ* XAS and XRD under severe abuse conditions at a cutoff voltage of 10 V and a temperature of 30 °C and 50 °C.

Development of strain/stress inside of the active electrode material can be an origin of performance degradation, leading to stress-induced damage and the formation of cracks [88-90]. Singer *et al.* [91] used the *in situ* Bragg coherent diffractive imaging (BCDI) technique to delineate three dimensional (3D) displacement fields inside of NCA and Li-rich layered oxides. BCDI can yield 3D images of strain from within a nanocrystal at high resolution [92]. Figure 3 b and c presents displacement and strain along 001 direction developed inside a single NCA particle during a charge.

During a cycle, TMs in LiTMO₂ take part in redox reactions to compensate charge imbalance induced by Li⁺ movements. In the case of NCA, Ni ions are mostly responsible for this phenomenon. Thus, tracking changes in valence of Ni ions can provide an insight in kinetics of Li⁺ during electrochemical reactions. Nowack *et al.* [50] visualized the state of charge (SOC) of NCA using *operando* full-field microscopy-based XAS. Figure 4 presents SOC mapping acquired with the Ni K-edge of NCA during electrochemical cycles in the range of 2.8-4.3 V. In order to minimize radiation dose and realize fast acquisition, 12 discrete energies were used for full-field TXM.

Furthermore, morphological changes of NCA during charge/discharge were visualized using a micro-battery set up inside of a scanning electron microscope (SEM) (Figure 5a) [93]. The battery system was composed of a Li₄Ti₅O₁₂ anode, 0.5 mol LiTFSI in P₁₃ TFSI electrolyte, and a single NCA particle as the cathode. External contacts were attached to both positive and negative electrodes *via* feedthroughs into the SEM. Figure 5b shows a series of SEM images acquired during the first charge, demonstrating an intergranular separation with lithium removal.

From these *in situ/operando* studies, we can summarize the following information: i) phase transformations occur within hexagonal systems, ii) charge and discharge mostly takes place with redox reaction of Ni ions, iii) lithium movement can induce the formation of cracks, which is consistent with *ex-situ* studies [9,94,95].

However, the mechanism of phase transformations is still controversial (i.e. whether it proceeds via solid solution *vs.* via a two-phase reaction). Thus, *operando* studies that probe these phenomena at the atomic scale are greatly needed.

4. *In situ* studies for investigating thermal degradation mechanism of charged NCA

It has been proposed that thermal runaway can occur spontaneously in LIBs above 80 °C, initiating with the decomposition of the solid electrolyte interphase (SEI) layer on the anode [96,97]. Heat generated from the breakdown of the SEI subsequently induces a reaction between the intercalated Li and the organic solvent. As a result of the exothermic nature of these reactions, the polymer separator can melt around 130 °C, resulting in a short-circuit between positive and negative electrodes [97]. This short-circuit may bring about an instantaneous temperature rise above 250 °C in the electrolyte [96], which is close to the temperature that breakdown of the cathode can be initiated. The decomposition of the cathode is highly exothermic and provokes liberation of oxygen, which can then react with the flammable organic electrolyte and eventually result in a catastrophic explosion. Thus, the thermal stability of cathode materials should be evaluated over a wide range of temperatures.

Ni-rich cathode materials have an even greater thermal instability, which further complicates widespread usage. This is because when they are in a highly delithiated state unstable Ni⁴⁺ has a tendency to reduce to the more stable Ni²⁺ state at high temperatures. This in turn releases oxygen

from the structure, which can accelerate thermal runaway [85,98,99]. Ni reduction is correlated with phase transitions to spinel and rocksalt structures (Figure 1), and thus obtaining XRD or electron diffraction patterns with increasing temperature is a valid approach to follow these processes. In order to investigate thermal degradation mechanisms, NCA positive electrodes was generally charged in a battery to a certain voltage or SOCs, then those delithiated NCA particles were acquired by disassembling a battery in a glove box. Thermal degradation of lithium nickel oxide derivatives [including NCA] was studied using *in situ* (time-resolved) XRD [100,101], and found that regardless of composition, a series of phase transition from layered to disordered spinel then to rocksalt occurs, with the onset temperature for the phase transitions being a function of both composition and SOCs. As the Ni content increases or as more lithium ions are removed, phase transformations occur at lower temperature, indicating poorer thermal stability. In order to probe structural changes and gas evolution at the same time, a new technique of *in situ* XRD coupled with mass spectroscopy (MS) was developed [56,102]. Figure 6 shows *in situ* XRD patterns with MS acquired from charged $\text{Li}_{0.5}\text{NCA}$ (i.e. 50% of Li was electrochemically removed). Upon heating, phase transformation from $\text{R}\bar{3}\text{m}$ layered structure to $\text{Fd}\bar{3}\text{m}$ (disordered spinel) and $\text{Fm}\bar{3}\text{m}$ (rocksalt) structures occurred, accompanied by O_2 and CO_2 release [102], demonstrating that phase transformation is directly correlated with the liberation of O_2 and CO_2 gases. In case of overcharged $\text{Li}_{0.1}\text{NCA}$ (only 10% of Li remaining), a severe oxygen release was observed with phase transformation to the disordered spinel phase around 175 °C, which is not high enough to ensure the safety of LIBs.

Along with *in situ* XRD, Yoon *et al.* [103] exploited the *in situ* soft XAS technique to investigate the thermal behavior of charged NCA ($\text{Li}_{0.33}\text{NCA}$). Soft XAS can probe the valence state of each element with site-selectivity since the partial electron yield is surface sensitive (up to 5 nm) while,

in turn determine bulk behavior using fluorescent yield. X-ray diffraction patterns and Ni and Co $L_{2,3}$ edge and O K-edge XAS of $Li_{0.33}NCA$ were recorded with increasing temperature, demonstrating the formation of NiO-like rocksalt phase at the surface as a result of thermal degradation. Besli *et al.* [51] systematically investigated thermal decomposition, oxygen release, and fracture of chemically delithiated NCA ($Li_{0.3}NCA$) with *in situ* XRD, soft XAS, *in situ* full-field TXM, and SEM upon heating. Figure 7 exhibits *in situ* 2D Ni K-edge XANES maps, which provide images of the spatial distribution of Ni oxidation states over an isolated secondary $Li_{0.3}NCA$ particle during a temperature excursion from room temperature to 450 °C. Significant Ni reduction was observed upon the transition from 200 °C to 250 °C and from 300 °C to 350 °C. It was suggested that oxygen evolution, phase transformations, reduction of Ni, intragranular cracking, and the development of mesopores all take place within delithiated NCA at high temperature.

The degree of lithium removal at the surface of electrode materials can be higher than that at the bulk, even at the same SOC because of slow lithium diffusion and overpotential at the interface between electrode-electrolyte. Structural inhomogeneity of charged NCA has been demonstrated at the nanoscale after the initial charge: specifically vis the presence of disordered spinel and rocksalt phases at the surface of $Li_{0.5}NCA$ and $Li_{0.1}NCA$ [104]. This structural variation may bring about unexpected thermal decomposition of charged NCA. As a result, Hwang *et al.* [105] investigated thermally induced decomposition occurring in charged NCA as a function of different SOC's using *in situ* TEM. Figure 8 presents a series of bright-field images, O K-edge EELS, and selected area electron diffraction (SAED) patterns acquired from charged NCA upon heating to 400 °C. Porosity developed at the surface then propagated into the bulk, suggesting oxygen evolution initiated at the surface then spread into the interior of the particles. This morphological

evolution took place along with crystallographic and electronic structural changes, as reflected in EELS and SAED data. In addition, thanks to site-specificity of TEM analysis, particle-to-particle variation in thermal behavior was examined through investigating of different particles at $\text{Li}_{0.33}\text{NCA}$, suggesting that localized area can undergo severe degradation even below 100 C, which is the temperature can be reached in normal operation. Karki *et al.* [106] explored the effect of environments on thermal degradation of overcharged $\text{Li}_{0.1}\text{NCA}$ using environmental TEM. Oxidizing, neutral, or reducing environment were controlled by introducing O_2 , He, H_2 gas into the sample area inside ETEM. Surface oxygen loss and structural changes were suppressed with O_2 environment while greatly accelerated under H_2 .

Thermal degradation of NCA was also examined *in situ* in the charged state using both X-ray based techniques and TEM. At comparable SOC, thermal degradation was observed at lower temperature in TEM since TEM probes a localized surface area, where is subjected to more severe delithiation. This indicates that thermal degradation initiates at the surface of cathode material at lower temperatures then subsequently propagates into bulk areas at high temperatures.

5. Outlook and summary

Lithium nickel cobalt aluminum oxides have been improved in order to simultaneously achieve high-energy density and enhanced structural stability. Research and development efforts have been also been pursued to use more than 80% of Ni in NCA to attain high capacity. The conflicting effect of increasing Ni content – it is good for high capacity but unfavorable to maintain a static crystal structure – can perhaps be mitigated with smart designs of novel material forms. For example, a concentration gradient $\text{LiNi}_{0.865}\text{Co}_{0.120}\text{Al}_{0.015}\text{O}_2$ was designed where the composition of TM within the bulk of the particle is Ni-rich while maintaining a Co-rich surface [107]. In

addition, a hybrid $\text{LiNi}_{0.886}\text{Co}_{0.049}\text{Mn}_{0.050}\text{Al}_{0.015}\text{O}_2$ has been proposed, consisting of a core of $\text{LiNi}_{0.934}\text{Co}_{0.043}\text{Al}_{0.015}\text{O}_2$ and an encapsulating shell of $\text{LiNi}_{0.844}\text{Co}_{0.080}\text{Al}_{0.015}\text{O}_2$ [108]. In other words, NCA-derivatives continue to be upgraded, even after successful commercialization, as they are highly promising positive electrode for EV applications. For exploring potential new chemistries of cathode materials, machine learning algorithms can be intriguing to predict the atomic configuration of novel materials during delithiation [109]. It is also desirable that materials development be correlated with *in situ/operando* characterization as they advance our understanding in structural and chemical evolution of NCA materials during operation. For example, an *in situ* study on structural evolution during synthesis of high-Ni content layered oxides may shed light on rational design of high-Ni cathode materials [110,111].

Careful design of experiments is mandatory to link *in situ/operando* characterization with the performance of real-life lithium ion batteries. Experimental setups for *in situ/operando* XRD and XAS (hard X-rays) are relatively easy to be prepared but they have limitations in probing amorphous materials and low atomic number elements, respectively [49]. Soft X-ray XAS, TXM and TEM approaches require complicated *in situ* liquid cells to realize a micro-battery system. Despite the difficulties of fabricating a closed-cell system, it is intriguing platform to probe materials both in TEM and XAS with an identical setup [112]. *In situ* TEM holders continue to be upgraded to mimic the realistic conditions as closely as possible. For instance, a newly developed *in situ* liquid TEM holder allows us precise electrochemical measurements [113]. Additionally, beam effects must be carefully considered for *in situ/operando* studies. Charged NCA is unstable, and thus easily damaged by either X-ray or electron beams. In addition, identical areas of sample are exposed several times to X-ray and electron beams during *in situ* experiments, therefore, in order to deliver reliable results, radiation should be minimized.

In this review, various *in situ/ operando* analytical techniques that have been applied to probing NCA cathode materials have been described. These techniques are also applicable to the examination of other layered cathode materials such as $\text{LiNi}_x\text{Mn}_y\text{Co}_z\text{O}_2$ [42,114-116], lithium-rich materials [58,117-120] as well as other electrode materials for other battery systems, like Li-S [121-124] and Li-air batteries [125-129]. Multimodal *operando* analysis including both X-ray-based and electron microscopy-based techniques are highly recommended as they can more deeply probe the structural and chemical evolution of electrode materials at complementary length scales.

Acknowledgements

This work is supported by the Center for Functional Nanomaterials, which is a U.S. DOE Office of Science Facility, at Brookhaven National Laboratory under Contract No. DE-SC0012704.

1 Figures

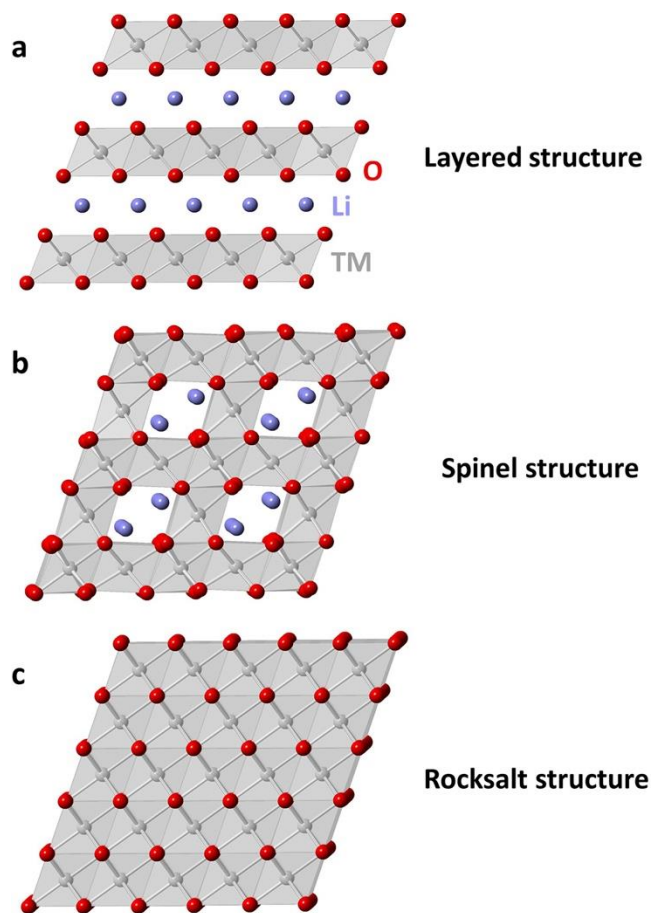


Figure 1. (a) Atomic model of pristine NCA. The original layered structure can be transformed to (b) spinel and (c) rocksalt structures after a number of cycles or at high temperatures.

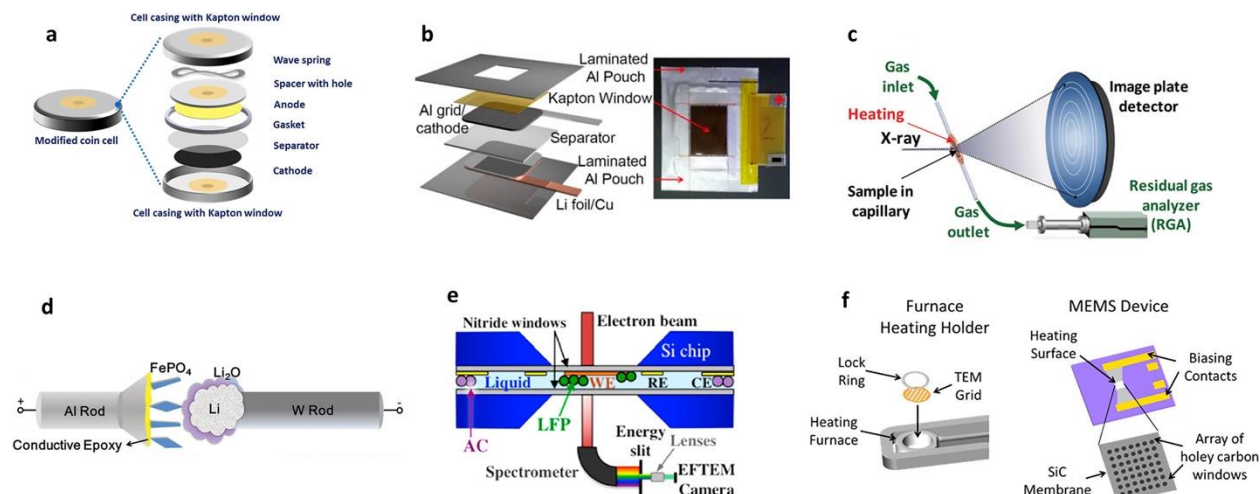


Figure 2. Schematics of experimental setups. Modified (a) coin cell and (b) pouch cell for in-situ/operando X-ray analysis. (c) Combination of X-ray diffraction and mass spectroscopy with heating. (d) Dry cell and (e) liquid cell and for in-situ lithiation/ delithiation inside TEM. (f) In-situ heating devices for TEM. (a) Reprinted with permission from [49]. Copyright © (2018) Springer Nature. (b) Reprinted with permission from [130]. Copyright © (2015) Wiley-VCH. (c) Reprinted with permission from [56]. Copyright © (2012) Wiley-VCH. (d) Reprinted with permission from [72]. Copyright © (2013) Wiley-VCH. (e) Reprinted with permission from [75]. Copyright © (2014) American Chemical Society. (f) Reprinted with permission from [80]. Copyright © (2018) American Chemical Society.

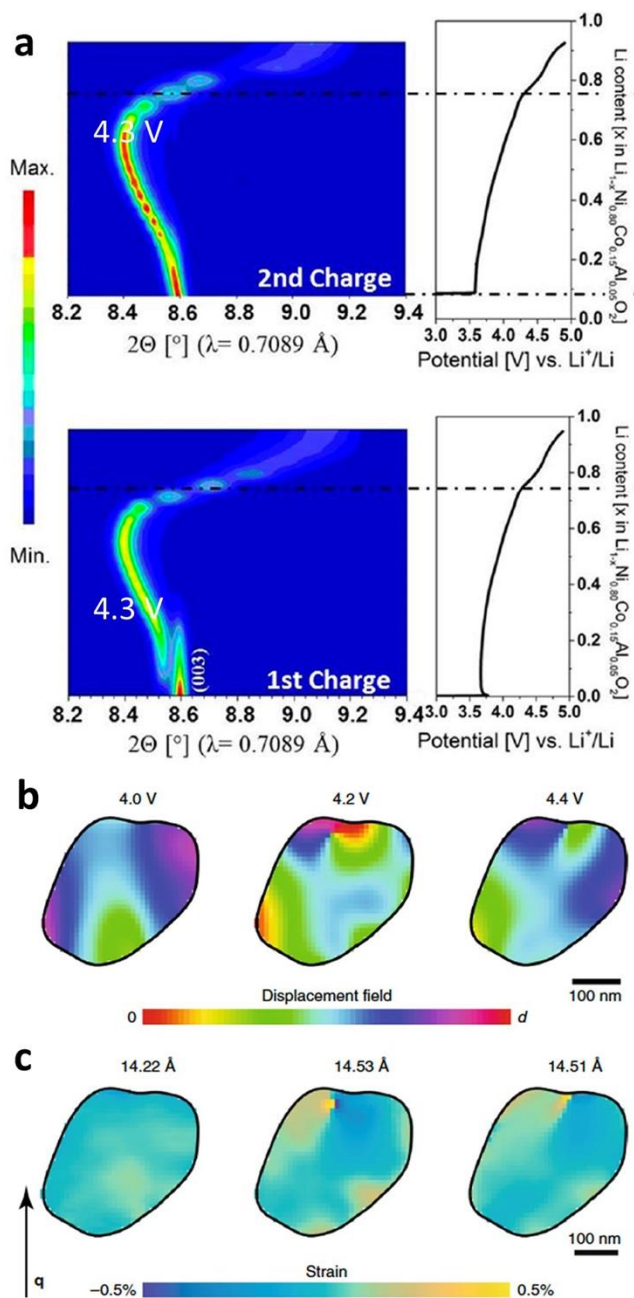


Figure 3. (a) Contour plots of the intensity at selected 2θ regions and corresponding galvanostatic plots of NCA for the first and second charge to 4.9 V Li^+/Li . (b) Displacement field (c) and strain along the (001) direction (perpendicular to the layers) of a single NCA particle captured in situ during charge. The voltages and average lattice constants are indicated. (a) Reprinted with permission from [82]. Copyright © (2015) American Chemical Society. (b, c) Reprinted with permission from [91]. Copyright © (2018) Springer Nature.

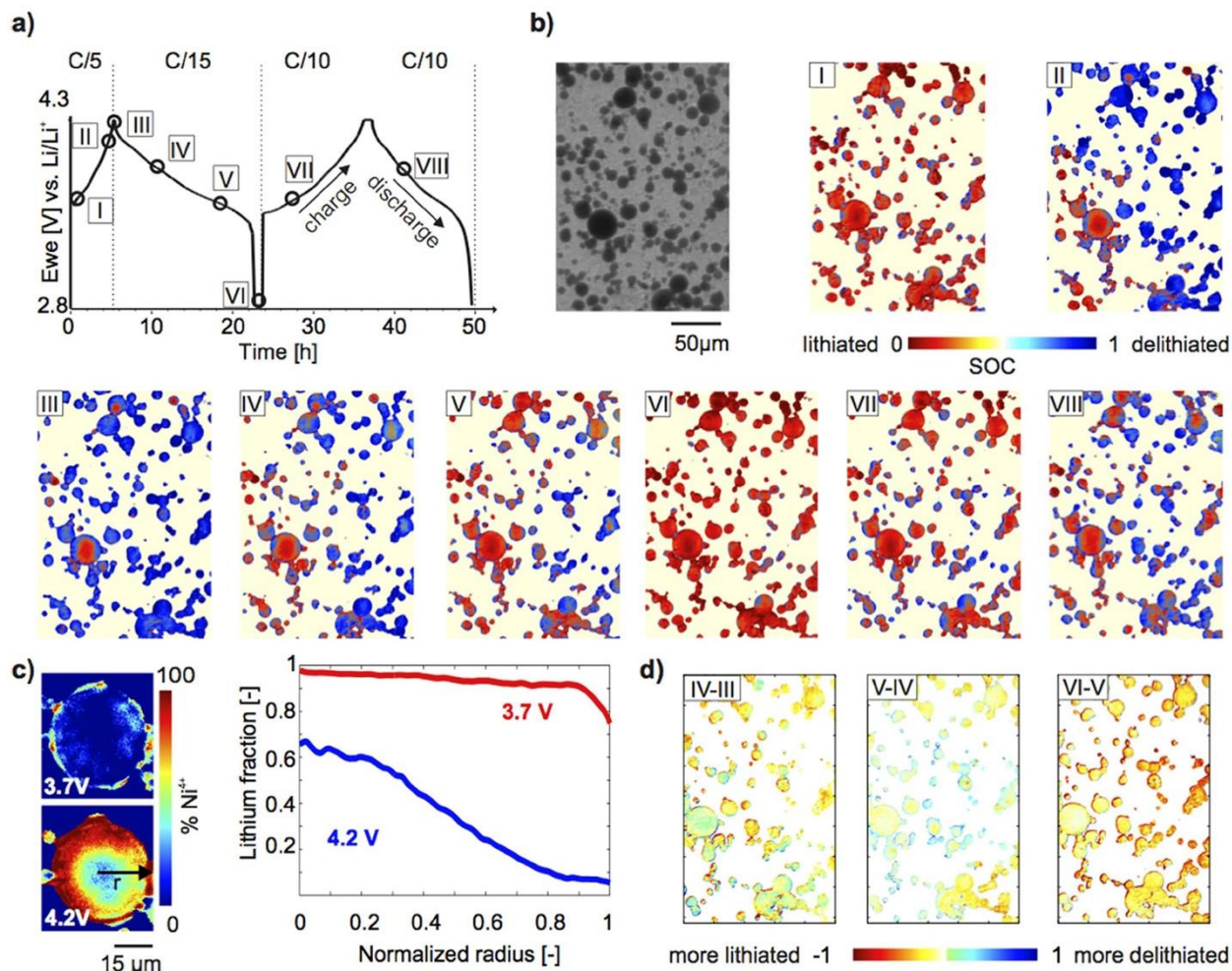


Figure 4. State of charge (SOC) mapping during electrochemical cycling. (a) Electrochemical cycling profile. (b) Transmission image of a region of electrode for which SOC maps for points I–VIII during the electrochemical cycle shown in panel (a). False color indicates extent of lithiation (red) or delithiation (blue). (c) Left: Ni^{4+} oxidation maps of a single large particle during charge at 3.7 V and 4.2 V (times steps I and II in panel (a)). A ring-like delithiation pattern is already visible at 3.7 V. Right: Radially integrated fraction of lithium in the particle at 3.7 V and 4.2 V as a function of distance from the center of the particle ($r = 0$) showing inhomogeneous lithiation in large particles at C/5. (d) Map of the difference in lithium content between the sequential timesteps III and IV (left), IV and V (middle), and V and VI (right). Reprinted with permission from [50]. Copyright © (2016) Springer Nature.

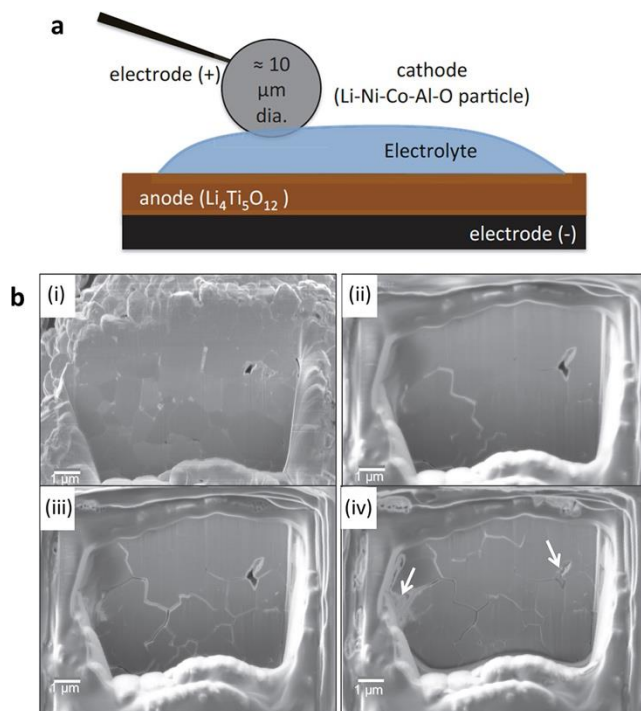


Figure 5. (a) Schematic representation of a microscale battery implemented in a scanning electron microscope for in situ studies of microstructural evolution. The battery consists of a single cathode particle partially immersed in electrolyte that covers the anode material. External leads are attached to the positive and negative electrodes via feedthroughs for electrochemical cycling. (b) A series of still images from live video collected during the first charge of a NCA particle. i) The polished surface within a single particle in the as-prepared condition just prior to final polishing and cycling, ii) about one third, iii) about two thirds and iv) at the end of the first charge cycle. In d) the electrolyte penetration to the interior of the particle can be observed (indicated by the two arrowed regions). (a) Reprinted with permission from [93]. Copyright © (2012) Microscopy Society of America. (b) Reprinted with permission from [131]. Copyright © (2013) Wiley-VCH.

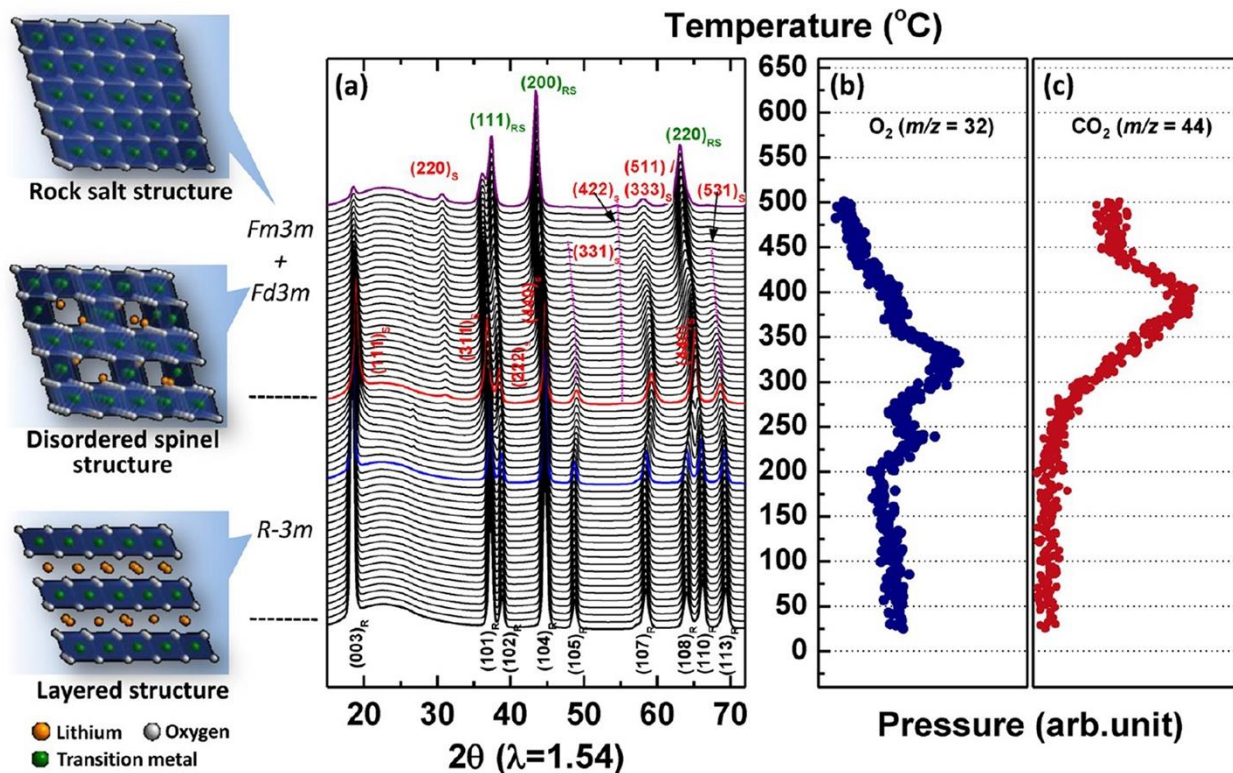


Figure 6. (a) TR-XRD patterns and simultaneously measured mass spectra (MS) for (b) O_2 and (c) CO_2 , released from $Li_{0.5}NCA$ during heating to 500 °C. The left panel shows the models of ideal crystals with rhombohedral, spinel, and rock-salt structures. Reprinted with permission from [102]. Copyright © (2013) American Chemical Society.

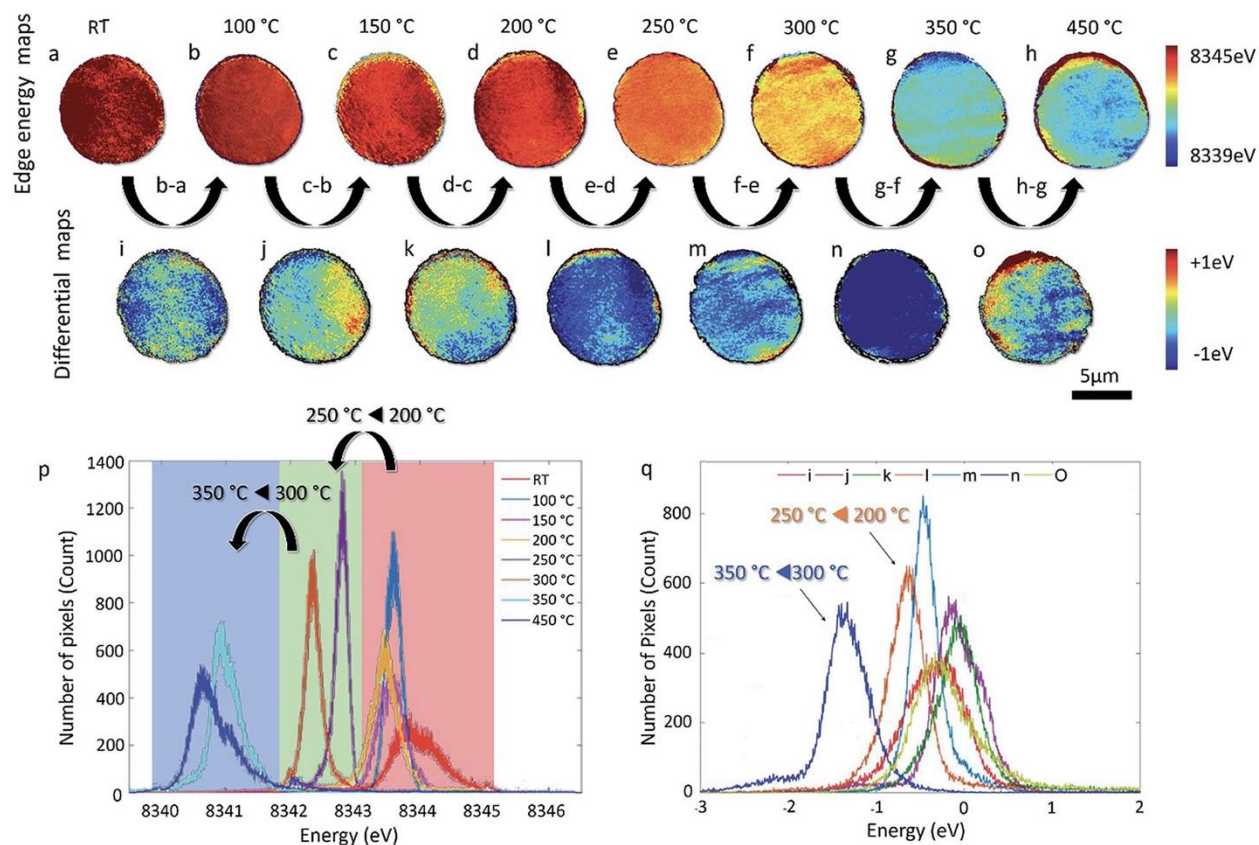


Figure 7. *In situ* 2D Ni K-edge XANES mapping over an arbitrarily selected NCA particle upon thermal treatment. Panels (a–h) show the evolution (reduction) of the Ni oxidation state. The corresponding energy distributions of panels (a–h) are shown in panel (p), highlighting two critical temperature transitions (200–250 °C and 300–350 °C). Panels (i–o) show the differential Ni K-edge energy maps, suggesting that the internal redistribution of Li occurs concurrently with the overall Ni reduction. The corresponding energy distributions of panels (i–o) are shown in panel (q). Reprinted with permission from [51]. Copyright © (2019) Royal Society of Chemistry.

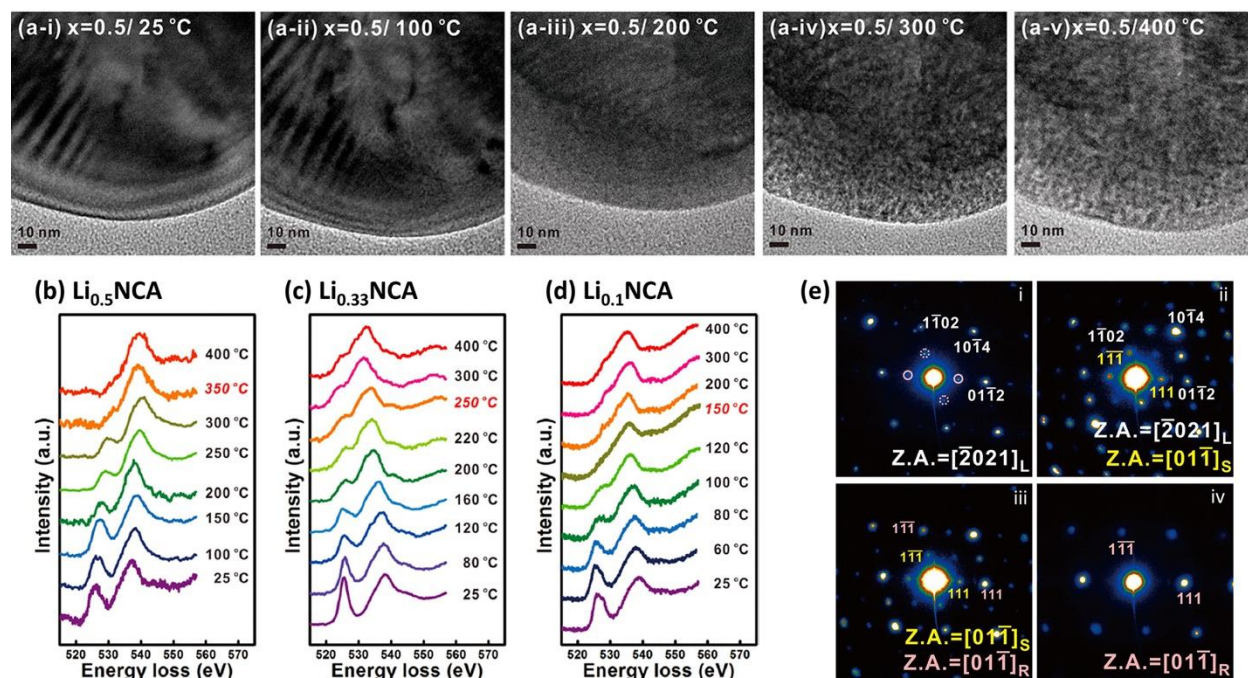


Figure 8. Real-time BF images of the surface of (row a) $\text{Li}_{0.5}\text{NCA}$ during heating. Temperature dependence of oxygen K-edge EEL spectra from (b) $\text{Li}_{0.5}\text{NCA}$, (c) $\text{Li}_{0.33}\text{NCA}$, and (d) $\text{Li}_{0.1}\text{NCA}$. (e) In-situ selected electron diffraction pattern acquired from $\text{Li}_{0.5}\text{NCA}$ at i) 25°C , ii) 200°C , iii) 300°C , and iv) 400°C . Reprinted with permission from [105]. Copyright © (2014) American Chemical Society.

References

- [1] <https://www.nobelprize.org/prizes/chemistry/2019/summary/>
- [2] Ozawa K 1994 Lithium-ion rechargeable batteries with LiCoO₂ and carbon electrodes: the LiCoO₂/C system *Solid State Ionics* **69** 212–21
- [3] Whittingham M S 2004 Lithium Batteries and Cathode Materials *Chem. Rev.* **104** 4271–301
- [4] Goodenough J B and Kim Y 2010 Challenges for Rechargeable Li Batteries *Chem. Mater.* **22** 587–603
- [5] Delmas C, Saadoun I and Rougier A 1993 The cycling properties of the Li_xNi_{1-y}CO_yO₂ electrode *J. Power Sources* **43-44** 595–602
- [6] Saadoun I and Delmas C 1996 LiNi_{1-y}Co_yO₂ positive electrode materials: relationships between the structure, physical properties and electrochemical behaviour *J. Mater. Chem.* **6** 193–9
- [7] Cho J, Jung H, Park Y, Kim G and Lim H S 2000 Electrochemical Properties and Thermal Stability of Li_aNi_{1-x}Co_xO₂ Cathode Materials *J. Electrochem. Soc.* **147** 15–20
- [8] Guilnard M, Rougier A, Grüne M, Croguennec L and Delmas C 2003 Effects of aluminum on the structural and electrochemical properties of LiNiO₂ *J. Power Sources* **115** 305–14
- [9] Guilnard M 2003 Structural and electrochemical properties of LiNi_{0.70}Co_{0.15}Al_{0.15}O₂ *Solid State Ionics* **160** 39–50
- [10] Cao H, Xia B, Xu N and Zhang C 2004 Structural and electrochemical characteristics of Co and Al co-doped lithium nickelate cathode materials for lithium-ion batteries *J. Alloys Compd.* **376** 282–6
- [11] Jo M, Noh M, Oh P, Kim Y and Cho J 2014 A New High Power LiNi_{0.81}Co_{0.1}Al_{0.09}O₂ Cathode Material for Lithium-Ion Batteries *Adv. Energy Mater.* **4** 1301583–8
- [12] Chen C H, Liu J, Stoll M E, Henriksen G, Vissers D R and Amine K 2004 Aluminum-doped lithium nickel cobalt oxide electrodes for high-power lithium-ion batteries *J. Power Sources* **128** 278–85
- [13] Myung S-T, Maglia F, Park K-J, Yoon C S, Lamp P, Kim S-J and Sun Y-K 2017 Nickel-Rich Layered Cathode Materials for Automotive Lithium-Ion Batteries: Achievements and Perspectives *ACS Energy Lett.* **2** 196–223

- [14] Schmuch R, Wagner R, Hörpel G, Placke T and Winter M 2018 Performance and cost of materials for lithium-based rechargeable automotive batteries *Nat. Energy* **3** 267–78
- [15] Watanabe S, Kinoshita M and Nakura K 2014 Capacity fade of $\text{LiNi}_{(1-x-y)}\text{Co}_x\text{Al}_y\text{O}_2$ cathode for lithium-ion batteries during accelerated calendar and cycle life test. I. Comparison analysis between $\text{LiNi}_{(1-x-y)}\text{Co}_x\text{Al}_y\text{O}_2$ and LiCoO_2 cathodes in cylindrical lithium-ion cells during long term storage test *J. Power Sources* **247** 412–22
- [16] Liu H, Wolf M, Karki K, Yu Y-S, Stach E A, Cabana J, Chapman K W and Chupas P J 2017 Intergranular Cracking as a Major Cause of Long-Term Capacity Fading of Layered Cathodes *Nano Lett.* **17** 3452–7
- [17] Lim B-B, Myung S-T, Yoon C S and Sun Y-K 2016 Comparative Study of Ni-Rich Layered Cathodes for Rechargeable Lithium Batteries: $\text{Li}[\text{Ni}_{0.85}\text{Co}_{0.11}\text{Al}_{0.04}]\text{O}_2$ and $\text{Li}[\text{Ni}_{0.84}\text{Co}_{0.06}\text{Mn}_{0.09}\text{Al}_{0.01}]\text{O}_2$ with Two-Step Full Concentration Gradients *ACS Energy Lett.* **1** 283–9
- [18] Abraham D P, Twesten R D, Balasubramanian M, Petrov I, McBreen J and Amine K 2002 Surface changes on $\text{LiNi}_{0.8}\text{Co}_{0.2}\text{O}_2$ particles during testing of high-power lithium-ion cells *Electrochem. Commun.* **4** 620–5
- [19] Abraham D P, Twesten R D, Balasubramanian M, Kropf J, Fischer D, McBreen J, Petrov I and Amine K 2003 Microscopy and Spectroscopy of Lithium Nickel Oxide-Based Particles Used in High Power Lithium-Ion Cells *J. Electrochem. Soc.* **150** A1450–6
- [20] Zheng S, Huang R, Makimura Y, Ukyo Y, Fisher C A J, Hirayama T and Ikuhara Y 2011 Microstructural Changes in $\text{LiNi}_{0.8}\text{Co}_{0.15}\text{Al}_{0.05}\text{O}_2$ Positive Electrode Material during the First Cycle *J. Electrochem. Soc.* **158** A357–62
- [21] Yano A, Aoyama S, Shikano M, Sakaebe H, Tatsumi K and Ogumi Z 2014 Surface Structure and High-Voltage Charge/Discharge Characteristics of Al-Oxide Coated $\text{LiNi}_{1/3}\text{Co}_{1/3}\text{Mn}_{1/3}\text{O}_2$ Cathodes *J. Electrochem. Soc.* **162** A3137–44
- [22] Jung S-K, Gwon H, Hong J, Park K-Y, Seo D-H, Kim H, Hyun J, Yang W and Kang K 2014 Understanding the Degradation Mechanisms of $\text{LiNi}_{0.5}\text{Co}_{0.2}\text{Mn}_{0.3}\text{O}_2$ Cathode Material in Lithium Ion Batteries *Adv. Energy Mater.* **4** 1300787
- [23] Lin F, Nordlund D, Markus I M, Weng T-C, Xin H L and Doeff M M 2014 Profiling the nanoscale gradient in stoichiometric layered cathode particles for lithium-ion batteries *Energy Environ. Sci.* **7** 3077–85
- [24] Gu M, Belharouak I, Zheng J, Wu H, Xiao J, Genc A, Amine K, Thevuthasan S, Baer D R, Zhang J-G, Browning N D, Liu J and Wang C 2013 Formation of the Spinel Phase in the Layered Composite Cathode Used in Li-Ion Batteries *ACS Nano* **7** 760–7

- [25] Striebel K A, Shim J, Cairns E J, Kostecki R, Lee Y J, Reimer J, Richardson T J, Ross P N, Song X and Zhuang G V 2004 Diagnostic Analysis of Electrodes from High-Power Lithium-Ion Cells Cycled under Different Conditions *J. Electrochem. Soc.* **151** A857
- [26] Andersson A M, Abraham D P, Haasch R, MacLaren S, Liu J and Amine K 2002 Surface Characterization of Electrodes from High Power Lithium-Ion Batteries *J. Electrochem. Soc.* **149** A1358
- [27] Muto S, Sasano Y, Tatsumi K, Sasaki T, Horibuchi K, Takeuchi Y and Ukyo Y 2009 Capacity-Fading Mechanisms of LiNiO₂-Based Lithium-Ion Batteries *J. Electrochem. Soc.* **156** A371–7
- [28] Kojima Y, Muto S, Tatsumi K, Kondo H, Oka H, Horibuchi K and Ukyo Y 2011 Degradation analysis of a Ni-based layered positive-electrode active material cycled at elevated temperatures studied by scanning transmission electron microscopy and electron energy-loss spectroscopy *J. Power Sources* **196** 7721–7
- [29] Kerlau M, Marcinek M, Srinivasan V and Kostecki R M 2007 Studies of local degradation phenomena in composite cathodes for lithium-ion batteries *Electrochim. Acta* **52** 5422–9
- [30] Kobayashi H, Emura S, Arachi Y and Tatsumi K 2007 Investigation of inorganic compounds on the surface of cathode materials using Li and O K-edge XANES *J. Power Sources* **174** 774–8
- [31] Waldmann T, Iturrondobeitia A, Kasper M, Ghanbari N, Aguesse F, Bekaert E, Daniel L, Genies S, Gordon I J, Löble M W, De Vito E and Wohlfahrt-Mehrens M 2016 Review—Post-Mortem Analysis of Aged Lithium-Ion Batteries: Disassembly Methodology and Physico-Chemical Analysis Techniques *J. Electrochem. Soc.* **163** A2149–64
- [32] Somerville L, Bareño J, Jennings P, McGordon A, Lyness C and Bloom I 2016 The Effect of Pre-Analysis Washing on the Surface Film of Graphite Electrodes *Electrochim. Acta* **206** 70–6
- [33] Huang W, Marcelli A and Xia D 2017 Application of Synchrotron Radiation Technologies to Electrode Materials for Li- and Na-Ion Batteries *Adv. Energy Mater.* **7** 1700460–31
- [34] Chen Z, Ren Y, Lee E, Johnson C, Qin Y and Amine K 2013 Study of Thermal Decomposition of Li_{1-x}(Ni_{1/3}Mn_{1/3}Co_{1/3})_{0.9}O₂ Using In-Situ High-Energy X-Ray Diffraction *Adv. Energy Mater.* **3** 729–36
- [35] Zhou Y-N, Yue J-L, Hu E, Li H, Gu L, Nam K-W, Bak S-M, Yu X, Liu J, Bai J, Dooryhee E, Fu Z-W and Yang X-Q 2016 High-Rate Charging Induced Intermediate Phases and Structural Changes of Layer-Structured Cathode for Lithium-Ion Batteries *Adv. Energy Mater.* **6** 1600597–8

- [36] Hirayama M, Ido H, Kim K, Cho W, Tamura K, Mizuki J and Kanno R 2010 Dynamic Structural Changes at LiMn_2O_4 /Electrolyte Interface during Lithium Battery Reaction *J. Am. Chem. Soc.* **132** 15268–76
- [37] Wiaderek K M, Borkiewicz O J, Castillo-Martínez E, Robert R, Pereira N, Amatucci G G, Grey C P, Chupas P J and Chapman K W 2013 Comprehensive Insights into the Structural and Chemical Changes in Mixed-Anion FeOF Electrodes by Using Operando PDF and NMR Spectroscopy *J. Am. Chem. Soc.* **135** 4070–8
- [38] Wang F, Robert R, Chernova N A, Pereira N, Omenya F, Badway F, Hua X, Ruotolo M, Zhang R, Wu L, Volkov V, Su D, Key B, Whittingham M S, Grey C P, Amatucci G G, Zhu Y and Graetz J 2011 Conversion Reaction Mechanisms in Lithium Ion Batteries: Study of the Binary Metal Fluoride Electrodes *J. Am. Chem. Soc.* **133** 18828–36
- [39] Zeng D, Cabana J, Bréger J, Yoon W-S and Grey C P 2007 Cation Ordering in $\text{Li}[\text{Ni}_x\text{Mn}_x\text{Co}_{(1-2x)}]\text{O}_2$ -Layered Cathode Materials: A Nuclear Magnetic Resonance (NMR), Pair Distribution Function, X-ray Absorption Spectroscopy, and Electrochemical Study *Chem. Mater.* **19** 6277–89
- [40] Takamatsu D, Koyama Y, Orikasa Y, Mori S, Nakatsutsumi T, Hirano T, Tanida H, Arai H, Uchimoto Y and Ogumi Z 2012 First In Situ Observation of the LiCoO_2 Electrode/Electrolyte Interface by Total-Reflection X-ray Absorption Spectroscopy *Angew. Chem. Int. Ed.* **51** 11597–601
- [41] Lin F, Markus I M, Nordlund D, Weng T-C, Asta M D, Xin H L and Doeff M M 2014 Surface reconstruction and chemical evolution of stoichiometric layered cathode materials for lithium-ion batteries *Nat. Commun.* **5** 3529
- [42] Tsai Y W, Hwang B J, Ceder G, Sheu H S, Liu D G and Lee J F 2005 In-Situ X-ray Absorption Spectroscopic Study on Variation of Electronic Transitions and Local Structure of $\text{LiNi}_{1/3}\text{Co}_{1/3}\text{Mn}_{1/3}\text{O}_2$ Cathode Material during Electrochemical Cycling *Chem. Mater.* **17** 3191–9
- [43] Yoon W-S, Balasubramanian M, Chung K Y, Yang X-Q, McBreen J, Grey C P and Fischer D A 2005 Investigation of the Charge Compensation Mechanism on the Electrochemically Li-Ion Deintercalated $\text{Li}_{1-x}\text{Co}_{1/3}\text{Ni}_{1/3}\text{Mn}_{1/3}\text{O}_2$ Electrode System by Combination of Soft and Hard X-ray Absorption Spectroscopy *J. Am. Chem. Soc.* **127** 17479–87
- [44] Deb A, Bergmann U, Cramer S P and Cairns E J 2005 In situ x-ray absorption spectroscopic study of the $\text{Li}[\text{Ni}_{1/3}\text{Co}_{1/3}\text{Mn}_{1/3}]\text{O}_2$ cathode material *J. Appl. Phys.* **97** 113523
- [45] Koningsberger D C and R P 1988 *X-ray Absorption: Principles, Applications, Techniques of EXAFS, SEXAFS and XANES* (New York: Wiley)

- [46] Chen-Wiegart Y-C K, Liu Z, Faber K T, Barnett S A and Wang J 2013 3D analysis of a $\text{LiCoO}_2\text{-Li}(\text{Ni}_{1/3}\text{Mn}_{1/3}\text{Co}_{1/3})\text{O}_2$ Li-ion battery positive electrode using x-ray nano-tomography *Electrochem. Commun.* **28** 127–30
- [47] Wang J, Chen-Wiegart Y-C K, Eng C, Shen Q and Wang J 2016 Visualization of anisotropic-isotropic phase transformation dynamics in battery electrode particles *Nat. Commun.* **7** 12372
- [48] Yang F, Liu Y, Martha S K, Wu Z, Andrews J C, Ice G E, Pianetta P and Nanda J 2014 Nanoscale Morphological and Chemical Changes of High Voltage Lithium–Manganese Rich NMC Composite Cathodes with Cycling *Nano Lett.* **14** 4334–41
- [49] Bak S-M, Shadik Z, Lin R, Yu X and Yang X-Q 2018 In situ/operando synchrotron-based X-ray techniques for lithium-ion battery research *NPG Asia Materials* **10** 563–80
- [50] Nowack L, Grolimund D, Samson V, Marone F and Wood V 2016 Rapid Mapping of Lithiation Dynamics in Transition Metal Oxide Particles with Operando X-ray Absorption Spectroscopy *Sci. Rep.* **6** 21479
- [51] Besli M M, Shukla A K, Wei C, Metzger M, Alvarado J, Boell J, Nordlund D, Schneider G, Hellstrom S, Johnston C, Christensen J, Doeff M M, Liu Y and Kuppan S 2019 Thermally-driven mesopore formation and oxygen release in delithiated NCA cathode particles *J. Mater. Chem. A* **7** 12593–603
- [52] Borkiewicz O J, Shyam B, Wiaderek K M, Kurtz C, Chupas P J and Chapman K W 2012 research papers The AMPIX electrochemical cell: a versatile apparatus for in situ X-ray scattering and spectroscopic measurements *J. Appl. Cryst* **45** 1261–9
- [53] Liu X, Wang D, Srinivasan V, Liu Z, Hussain Z, Liu G and Yang W 2013 Distinct charge dynamics in battery electrodes revealed by in situ and operando soft X-ray spectroscopy *Nat. Commun.* **4** 2568
- [54] Wang J, Eng C, Chen-Wiegart Y-C K and Wang J 2015 Probing three-dimensional sodiation-desodiation equilibrium in sodium-ion batteries by in situ hard X-ray nanotomography *Nat. Commun.* **6** 7496
- [55] Lim J, Li Y, Hein Alsem D, So H, Lee S C, Bai P, Cogswell D A, Liu X, Jin N, Yu Y-S, Salmon N J, Shapiro D A, Bazant M Z, Tyliszczak T and Chueh W C 2016 Origin and hysteresis of lithium compositional spatiodynamics within battery primary particles *Science* **353** 566–71
- [56] Nam K-W, Bak S-M, Hu E, Yu X, Zhou Y, Wang X, Wu L, Zhu Y, Chung K Y and Yang X-Q 2013 Combining In Situ Synchrotron X-Ray Diffraction and Absorption Techniques with Transmission Electron Microscopy to Study the Origin of Thermal Instability in Overcharged Cathode Materials for Lithium-Ion Batteries *Adv. Funct. Mater.* **23** 1047–63

- [57] Shao-Horn Y, Croguennec L, Delmas C, Nelson E C and O'Keeffe M A 2003 Atomic resolution of lithium ions in LiCoO_2 *Nat. Mater.* **2** 464–7
- [58] Sathiya M, Rouse G, Ramesha K, Laisa C P, Vezin H, Sougrati M T, Doublet M L, Foix D, Gonbeau D, Walker W, Prakash A S, Ben Hassine M, Dupont L and Tarascon J-M 2013 Reversible anionic redox chemistry in high-capacity layered-oxide electrodes *Nat. Mater.* **12** 827–35
- [59] Hwang S, Kim S M, Bak S-M, Chung K Y and Chang W 2015 Investigating the Reversibility of Structural Modifications of $\text{Li}_x\text{Ni}_y\text{Mn}_z\text{Co}_{1-y-z}\text{O}_2$ Cathode Materials during Initial Charge/Discharge, at Multiple Length Scales *Chem. Mater.* **27** 6044–52
- [60] Ahn J, Kim J H, Cho B-W, Chung K Y, Kim S, Choi J W and Oh S H 2017 Nanoscale Zirconium-Abundant Surface Layers on Lithium- and Manganese-Rich Layered Oxides for High-Rate Lithium-Ion Batteries *Nano Lett.* **17** 7869–77
- [61] Jo E, Hwang S, Kim S M and Chang W 2017 Investigating the Kinetic Effect on Structural Evolution of $\text{Li}_x\text{Ni}_{0.8}\text{Co}_{0.15}\text{Al}_{0.05}\text{O}_2$ Cathode Materials during the Initial Charge/Discharge *Chem. Mater.* **29** 2708–16
- [62] Zhang H, Karki K, Huang Y, Whittingham M S, Stach E A and Zhou G 2017 Atomic Insight into the Layered/Spinel Phase Transformation in Charged $\text{LiNi}_{0.80}\text{Co}_{0.15}\text{Al}_{0.05}\text{O}_2$ Cathode Particles *J. Phys. Chem. C* **121** 1421–30
- [63] Gu M, Belharouak I, Genc A, Wang Z, Wang D, Amine K, Gao F, Zhou G, Thevuthasan S, Baer D R, Zhang J-G, Browning N D, Liu J and Wang C 2012 Conflicting Roles of Nickel in Controlling Cathode Performance in Lithium Ion Batteries *Nano Lett.* **12** 5186–91
- [64] Yan P, Zheng J, Lv D, Wei Y, Zheng J, Wang Z, Kuppan S, Yu J, Luo L, Edwards D, Olszta M, Amine K, Liu J, Xiao J, Pan F, Chen G, Zhang J-G and Wang C-M 2015 Atomic-Resolution Visualization of Distinctive Chemical Mixing Behavior of Ni, Co, and Mn with Li in Layered Lithium Transition-Metal Oxide Cathode Materials *Chem. Mater.* **27** 5393–401
- [65] Kim H, Kim M-G, Jeong H Y, Nam H and Cho J 2015 A New Coating Method for Alleviating Surface Degradation of $\text{LiNi}_{0.6}\text{Co}_{0.2}\text{Mn}_{0.2}\text{O}_2$ Cathode Material: Nanoscale Surface Treatment of Primary Particles *Nano Lett.* **15** 2111–9
- [66] Xu B, Fell C R, Chi M and Meng Y S 2011 Identifying surface structural changes in layered Li-excess nickel manganese oxides in high voltage lithium ion batteries: A joint experimental and theoretical study *Energy Environ. Sci.* **4** 2223–33
- [67] Sathiya M, Abakumov A M, Foix D, Rouse G, Ramesha K, Sauranere M, Doublet M L, Vezin H, Laisa C P, Prakash A S, Gonbeau D, VanTendeloo G and Tarascon J-M 2015 Origin of voltage decay in high-capacity layered oxide electrodes *Nat. Mater.* **14** 230–8

- [68] Wang F, Yu H-C, Chen M-H, Wu L, Pereira N, Thornton K, Van der Ven A, Zhu Y, Amatucci G G and Graetz J 2012 Tracking lithium transport and electrochemical reactions in nanoparticles *Nat. Commun.* **3** 1201–8
- [69] Yan P, Zheng J, Wang Z, Teng G, Kuppan S, Xiao J, Chen G, Pan F, Zhang J-G and Wang C-M 2016 Ni and Co Segregations on Selective Surface Facets and Rational Design of Layered Lithium Transition-Metal Oxide Cathodes *Adv. Energy Mater.* **11** 1502455
- [70] Huang J Y, Zhong L, Wang C-M, Sullivan J P, Xu W, Zhang L Q, Mao S X, Hudak N S, Liu X H, Subramanian A, Fan H, Qi L, Kushima A and Li J 2010 In Situ Observation of the Electrochemical Lithiation of a Single SnO₂ Nanowire Electrode *Science* **330** 1515–20
- [71] Hwang S, Yao Z, Zhang L, Fu M, He K, Mai L, Wolverton C and Su D 2018 Multistep Lithiation of Tin Sulfide: An Investigation Using in Situ Electron Microscopy *ACS Nano* **12** 3638–45
- [72] Zhu Y, Wang J W, Liu Y, Liu X, Kushima A, Liu Y, Xu Y, Mao S X, Li J, Wang C and Huang J Y 2013 In Situ Atomic-Scale Imaging of Phase Boundary Migration in FePO₄ Microparticles During Electrochemical Lithiation *Adv. Mater.* **25** 5461–6
- [73] Kim S, Yao Z, Lim J-M, Hersam M C, Wolverton C, Dravid V P and He K 2018 Atomic-Scale Observation of Electrochemically Reversible Phase Transformations in SnSe₂ Single Crystals *Adv. Mater.* **30** 1804925–10
- [74] Gu M, Parent L R, Mehdi B L, Unocic R R, McDowell M T, Sacci R L, Xu W, Connell J G, Xu P, Abellan P, Chen X, Zhang Y, Perea D E, Evans J E, Lauhon L J, Zhang J-G, Liu J, Browning N D, Cui Y, Arslan I and Wang C-M 2013 Demonstration of an Electrochemical Liquid Cell for Operando Transmission Electron Microscopy Observation of the Lithiation/Delithiation Behavior of Si Nanowire Battery Anodes *Nano Lett.* **13** 6106–12
- [75] Holtz M E, Yu Y, Gunceler D, Gao J, Sundararaman R, Schwarz K A, Arias T A, Abruña H D and Muller D A 2014 Nanoscale Imaging of Lithium Ion Distribution During In Situ Operation of Battery Electrode and Electrolyte *Nano Lett.* **14** 1453–9
- [76] Leenheer A J, Jungjohann K L, Zavadil K R, Sullivan J P and Harris C T 2015 Lithium Electrodeposition Dynamics in Aprotic Electrolyte Observed in Situ via Transmission Electron Microscopy *ACS Nano* **9** 4379–89
- [77] Leenheer A J, Jungjohann K L, Zavadil K R and Harris C T 2016 Phase Boundary Propagation in Li-Alloying Battery Electrodes Revealed by Liquid-Cell Transmission Electron Microscopy *ACS Nano* **10** 5670–8
- [78] Lee S, Oshima Y, Hosono E, Zhou H, Kim K, Chang H M, Kanno R and Takayanagi K 2013 In Situ TEM Observation of Local Phase Transformation in a Rechargeable LiMn₂O₄ Nanowire Battery *J. Phys. Chem. C* **117** 24236–41

- [79] Gong Y, Zhang J, Jiang L, Shi J-A, Zhang Q, Yang Z, Zou D, Wang J, Yu X, Xiao R, Hu Y-S, Gu L, Li H and Chen L 2017 In Situ Atomic-Scale Observation of Electrochemical Delithiation Induced Structure Evolution of LiCoO₂ Cathode in a Working All-Solid-State Battery *J. Am. Chem. Soc.* **139** 4274–7
- [80] Veghte D P, China S, Weis J, Lin P, Hinks M L, Kovarik L, Nizkorodov S A, Gilles M K and Laskin A 2018 Heating-Induced Transformations of Atmospheric Particles: Environmental Transmission Electron Microscopy Study *Analytical Chemistry* **90** 9761–8
- [81] Yoon W-S, Chung K Y, McBreen J and Yang X-Q 2006 A comparative study on structural changes of LiCo_{1/3}Ni_{1/3}Mn_{1/3}O₂ and LiNi_{0.8}Co_{0.15}Al_{0.05}O₂ during first charge using in situ XRD *Electrochem. Commun.* **8** 1257–62
- [82] Robert R, Bünzli C, Berg E J and Novák P 2015 Activation Mechanism of LiNi_{0.80}Co_{0.15}Al_{0.05}O₂: Surface and Bulk Operando Electrochemical, Differential Electrochemical Mass Spectrometry, and X-ray Diffraction Analyses *Chem. Mater.* **27** 526–36
- [83] Grenier A, Liu H, Wiaderek K M, Lebens-Higgins Z W, Borkiewicz O J, Piper L F J, Chupas P J and Chapman K W 2017 Reaction Heterogeneity in LiNi_{0.8}Co_{0.15}Al_{0.05}O₂ Induced by Surface Layer *Chem. Mater.* **29** 7345–52
- [84] Chen Z, Qin Y, Ren Y, Lu W, Orendorff C, Roth E P and Amine K 2011 Multi-scale study of thermal stability of lithiated graphite *Energy Environ. Sci.* **4** 4023–8
- [85] Belharouak I, Vissers D and Amine K 2006 Thermal Stability of the Li(Ni_{0.8}Co_{0.15}Al_{0.05})O₂ Cathode in the Presence of Cell Components *J. Electrochem. Soc.* **153** A2030–5
- [86] Lin C-K, Ren Y, Amine K, Qin Y and Chen Z 2013 In situ high-energy X-ray diffraction to study overcharge abuse of 18650-size lithium-ion battery *J. Power Sources* **230** 32–7
- [87] Makimura Y, Sasaki T, Oka H, Okuda C, Nonaka T, Nishimura Y F, Kawauchi S and Takeuchi Y 2016 Studying the Charging Process of a Lithium-Ion Battery toward 10 V by In Situ X-ray Absorption and Diffraction: Lithium Insertion/Extraction with Side Reactions at Positive and Negative Electrodes *J. Electrochem. Soc.* **163** A1450–6
- [88] Wang H, Jang Y-I, Huang B, Sadoway D R and Chiang Y-M 1999 TEM Study of Electrochemical Cycling-Induced Damage and Disorder in LiCoO₂ Cathodes for Rechargeable Lithium Batteries *J. Electrochem. Soc.* **146** 473–80
- [89] Zhao K, Pharr M, Vlassak J J and Suo Z 2010 Fracture of electrodes in lithium-ion batteries caused by fast charging *J. Appl. Phys.* **108** 073517–7

- [90] Yan P, Zheng J, Gu M, Xiao J, Zhang J-G and Wang C-M 2017 Intragranular cracking as a critical barrier for high-voltage usage of layer-structured cathode for lithium-ion batteries *Nat. Commun.* **8** 14101
- [91] Singer A, Zhang M, Hy S, Cela D, Fang C, Wynn T A, Qiu B, Xia Y, Liu Z, Ulvestad A, Hua N, Wingert J, Liu H, Sprung M, Zozulya A V, Maxey E, Harder R, Meng Y S and Shpyrko O G 2018 Nucleation of dislocations and their dynamics in layered oxide cathode materials during battery charging *Nat. Energy* **3** 641–7
- [92] Chapman H N and Nugent K A 2010 Coherent lensless X-ray imaging *Nat. Photonics* **4** 833–9
- [93] Miller D J, Proff C, Wen J G and Abraham D J 2012 Direct Observation of Microstructural Evolution in Li Battery Cathode Oxide Particles during Electrochemical Cycling by in situ Electron Microscopy *Microsc. Microanal.* **18** 1108–9
- [94] Yoon W-S, Chung K Y, McBreen J, Fischer D A and Yang X-Q 2007 Electronic structural changes of the electrochemically Li-ion deintercalated $\text{LiNi}_{0.8}\text{Co}_{0.15}\text{Al}_{0.05}\text{O}_2$ cathode material investigated by X-ray absorption spectroscopy *J. Power Sources* **174** 1015–20
- [95] Watanabe S, Hosokawa T, Morigaki K, Kinoshita M and Nakura K 2012 Prevention of the Micro Cracks Generation in LiNiCoAlO_2 Cathode by the Restriction of ΔDOD *ECS Trans.* **41** 65–74
- [96] Hammami A, Raymond N and Armand M 2003 Runaway risk of forming toxic compounds *Nature* **424** 635–6
- [97] Wang Q, Ping P, Zhao X, Chu G, Sun J and Chen C 2012 Thermal runaway caused fire and explosion of lithium ion battery *J. Power Sources* **208** 210–24
- [98] Arai H, Okada S, Sakurai Y and Yamaki J-I 1998 Thermal behavior of $\text{Li}_{1-y}\text{NiO}_2$ and the decomposition mechanism *Solid State Ionics* **109** 295–302
- [99] Belharouak I, Lu W, Liu J, Vissers D and Amine K 2007 Thermal behavior of delithiated $\text{Li}(\text{Ni}_{0.8}\text{Co}_{0.15}\text{Al}_{0.05})\text{O}_2$ and $\text{Li}_{1.1}(\text{Ni}_{1/3}\text{Co}_{1/3}\text{Mn}_{1/3})_{0.9}\text{O}_2$ powders *J. Power Sources* **174** 905–9
- [100] Guilmard M, Croguennec L and Delmas C 2003 Thermal Stability of Lithium Nickel Oxide Derivatives. Part II: $\text{Li}_x\text{Ni}_{0.70}\text{Co}_{0.15}\text{Al}_{0.15}\text{O}_2$ and $\text{Li}_x\text{Ni}_{0.90}\text{Mn}_{0.10}\text{O}_2$ ($x=0.50$ and 0.30). Comparison with $\text{Li}_x\text{Ni}_{1.02}\text{O}_2$ and $\text{Li}_x\text{Ni}_{0.89}\text{Al}_{0.16}\text{O}_2$ *Chem. Mater.* **15** 4484–93
- [101] Yoon W-S, Chung K Y, Balasubramanian M, Hanson J, McBreen J and Yang X-Q 2006 Time-resolved XRD study on the thermal decomposition of nickel-based layered cathode materials for Li-ion batteries *J. Power Sources* **163** 219–22

- [102] Bak S-M, Nam K-W, Chang W, Yu X, Hu E, Hwang S, Stach E A, Kim K-B, Chung K Y and Yang X-Q 2013 Correlating Structural Changes and Gas Evolution during the Thermal Decomposition of Charged $\text{Li}_x\text{Ni}_{0.8}\text{Co}_{0.15}\text{Al}_{0.05}\text{O}_2$ Cathode Materials *Chem. Mater.* **25** 337–51
- [103] Yoon W-S, Haas O, Muhammad S, Kim H, Lee W, Kim D, Fischer D A, Jaye C, Yang X-Q, Balasubramanian M and Nam K-W 2014 In situ soft XAS study on nickel-based layered cathode material at elevated temperatures: A novel approach to study thermal stability *Sci. Rep.* **4** 6827
- [104] Hwang S, Chang W, Kim S M, Su D, Kim D H, Lee J Y, Chung K Y and Stach E A 2014 Investigation of Changes in the Surface Structure of $\text{Li}_x\text{Ni}_{0.8}\text{Co}_{0.15}\text{Al}_{0.05}\text{O}_2$ Cathode Materials Induced by the Initial Charge *Chem. Mater.* **26** 1084–92
- [105] Hwang S, Kim S M, Bak S-M, Cho B-W, Chung K Y, Lee J Y, Chang W and Stach E A 2014 Investigating the Local Degradation and Thermal Stability of Charged Ni-Based Cathode Materials through Real-Time Electron Microscopy *ACS Appl. Mater. Interfaces* **6** 15140–7
- [106] Karki K, Huang Y, Hwang S, Gamalski A D, Whittingham M S, Zhou G and Stach E A 2016 Tuning the Activity of Oxygen in $\text{LiNi}_{0.8}\text{Co}_{0.15}\text{Al}_{0.05}\text{O}_2$ Battery Electrodes *ACS Appl. Mater. Interfaces* **8** 27762–71
- [107] Park K-J, Choi M-J, Maglia F, Kim S-J, Kim K-H, Yoon C S and Sun Y-K 2018 High-Capacity Concentration Gradient $\text{Li}[\text{Ni}_{0.865}\text{Co}_{0.120}\text{Al}_{0.015}]\text{O}_2$ Cathode for Lithium-Ion Batteries *Adv. Energy Mater.* **8** 1703612–10
- [108] Kim U-H, Kim J-H, Hwang J-Y, Ryu H-H, Yoon C S and Sun Y-K 2019 Compositionally and structurally redesigned high-energy Ni-rich layered cathode for next-generation lithium batteries *Mater. Today* **23** 26–36
- [109] Eremin R A, Zolotarev P N, Ivanshina O Y and Bobrikov I A 2017 $\text{Li}(\text{Ni},\text{Co},\text{Al})\text{O}_2$ Cathode Delithiation: A Combination of Topological Analysis, Density Functional Theory, Neutron Diffraction, and Machine Learning Techniques *J. Phys. Chem. C* **121** 28293–305
- [110] Zhang M-J, Teng G, Chen-Wiegart Y-C K, Duan Y, Ko J Y P, Zheng J, Thieme J, Dooryhee E, Chen Z, Bai J, Amine K, Pan F and Wang F 2018 Cationic Ordering Coupled to Reconstruction of Basic Building Units during Synthesis of High-Ni Layered Oxides *J. Am. Chem. Soc.* **140** 12484–92
- [111] Zhang M-J, Hu X, Li M, Duan Y, Yang L, Yin C, Ge M, Xiao X, Lee W K, Ko J Y P, Amine K, Chen Z, Zhu Y, Dooryhee E, Bai J, Pan F and Wang F 2019 Cooling Induced Surface Reconstruction during Synthesis of High-Ni Layered Oxides *Adv. Energy Mater.* **29** 1901915–10
- [112] Li Y, Zakharov D, Zhao S, Tappero R, Jung U, Elsen A, Baumann P, Nuzzo R G, Stach E A and Frenkel A I 2015 Complex structural dynamics of nanocatalysts

revealed in Operando conditions by correlated imaging and spectroscopy probes
Nat. Commun. **6** 7583

- [113] <http://hummingbirdscientific.com/products/bulk-liquid-electrochemistry/>
- [114] Bak S-M, Hu E, Zhou Y, Yu X, Senanayake S D, Cho S-J, Kim K-B, Chung K Y, Yang X-Q and Nam K-W 2014 Structural Changes and Thermal Stability of Charged $\text{LiNi}_x\text{Mn}_y\text{Co}_z\text{O}_2$ Cathode Materials Studied by Combined In Situ Time-Resolved XRD and Mass Spectroscopy *ACS Appl. Mater. Interfaces* **6** 22594–601
- [115] Hwang S, Kim S M, Bak S-M, Kim S Y, Cho B-W, Chung K Y, Lee J Y, Stach E A and Chang W 2015 Using Real-Time Electron Microscopy To Explore the Effects of Transition-Metal Composition on the Local Thermal Stability in Charged $\text{Li}_x\text{Ni}_y\text{Mn}_z\text{Co}_{1-y-z}\text{O}_2$ Cathode Materials *Chem. Mater.* **27** 3927–35
- [116] Yan P, Zheng J, Chen T, Luo L, Jiang Y, Wang K, Sui M, Zhang J-G, Zhang S and Wang C 2018 Coupling of electrochemically triggered thermal and mechanical effects to aggravate failure in a layered cathode *Nat. Commun.* **9** 2437
- [117] Koga H, Croguennec L, Menetrier M, Mannesiez P, Weill F, Delmas C and Belin S 2014 Operando X-ray Absorption Study of the Redox Processes Involved upon Cycling of the Li-Rich Layered Oxide $\text{Li}_{1.20}\text{Mn}_{0.54}\text{Co}_{0.13}\text{Ni}_{0.13}\text{O}_2$ in Li Ion Batteries *J. Phys. Chem. C* **118** 5700–9
- [118] Ito A, Sato Y, Sanada T, Hatano M, Horie H and Ohsawa Y 2011 In situ X-ray absorption spectroscopic study of Li-rich layered cathode material $\text{Li}[\text{Ni}_{0.17}\text{Li}_{0.2}\text{Co}_{0.07}\text{Mn}_{0.56}]\text{O}_2$ *J. Power Sources* **196** 6828–34
- [119] Myeong S, Cho W, Jin W, Hwang J, Yoon M, Yoo Y, Nam G, Jang H, Han J-G, Choi N-S, Kim M-G and Cho J 2018 Understanding voltage decay in lithium-excess layered cathode materials through oxygen-centred structural arrangement *Nat. Commun.* **9** 3285
- [120] Li S, Lee S-J, Wang X, Yang W, Huang H, Swetz D S, Doriese W B, O’Neil G C, Ullom J N, Titus C J, Irwin K D, Lee H-K, Nordlund D, Pianetta P, Yu C, Qiu J, Yu X, Yang X-Q, Hu E, Lee J-S and Liu Y 2019 Surface-to-Bulk Redox Coupling through Thermally Driven Li Redistribution in Li- and Mn-Rich Layered Cathode Materials *J. Am. Chem. Soc.* **141** 12079–86
- [121] Cañas N A, Wolf S, Wagner N and Friedrich K A 2013 In-situ X-ray diffraction studies of lithium-sulfur batteries *J. Power Sources* **226** 313–9
- [122] Yu X, Pan H, Zhou Y, Northrup P, Xiao J, Bak S, Liu M, Nam K-W, Qu D, Liu J, Wu T and Yang X-Q 2015 Direct Observation of the Redistribution of Sulfur and Polysulfides in Li-S Batteries During the First Cycle by In Situ X-Ray Fluorescence Microscopy *Adv. Energy Mater.* **5** 1500072–6

- [123] Cuisinier M, Cabelguen P-E, Evers S, He G, Kolbeck M, Garsuch A, Bolin T, Balasubramanian M and Nazar L F 2013 Sulfur Speciation in Li-S Batteries Determined by Operando X-ray Absorption Spectroscopy *J. Phys. Chem. Lett.* **4** 3227–32
- [124] Kim H, Lee J T, Magasinski A, Zhao K, Liu Y and Yushin G 2015 In Situ TEM Observation of Electrochemical Lithiation of Sulfur Confined within Inner Cylindrical Pores of Carbon Nanotubes *Adv. Energy Mater.* **5** 1501306–7
- [125] Yao K P C, Kwabi D G, Quinlan R A, Mansour A N, Grimaud A, Lee Y-L, Lu Y-C and Shao-Horn Y 2013 Thermal Stability of Li_2O_2 and Li_2O for Li-Air Batteries: In Situ XRD and XPS Studies *J. Electrochem. Soc.* **160** A824–31
- [126] Ryan K R, Trahey L, Okasinski J S, Burrell A K and Ingram B J 2013 In situ synchrotron X-ray diffraction studies of lithium oxygen batteries *J. Mater. Chem. A* **1** 6915–5
- [127] Ganapathy S, Adams B D, Stenou G, Anastasaki M S, Goubitz K, Miao X-F, Nazar L F and Wagemaker M 2014 Nature of Li_2O_2 Oxidation in a Li- O_2 Battery Revealed by Operando X-ray Diffraction *J. Am. Chem. Soc.* **136** 16335–44
- [128] Zhong L, Mitchell R R, Liu Y, Gallant B M, Thompson C V, Huang J Y, Mao S X and Shao-Horn Y 2013 In Situ Transmission Electron Microscopy Observations of Electrochemical Oxidation of Li_2O_2 *Nano Lett.* **13** 2209–14
- [129] Luo L, Bin Liu, Song S, Xu W, Zhang J-G and Wang C 2017 Revealing the reaction mechanisms of Li- O_2 batteries using environmental transmission electron microscopy *Nat. Nanotechnol.* **12** 535–9
- [130] Ghanty C, Markovsky B, Erickson E M, Talianker M, Haik O, Tal-Yossef Y, Mor A, Aurbach D, Lampert J, Volkov A, Shin J-Y, Garsuch A, Chesneau F F and Erk C 2015 Li^+ -Ion Extraction/Insertion of Ni-Rich $\text{Li}_{1+x}(\text{Ni}_y\text{Co}_z\text{Mn}_z)_w\text{O}_2$ ($0.005 < x < 0.03$; $y: z = 8:1$, $w \approx 1$) Electrodes: In Situ XRD and Raman Spectroscopy Study *ChemElectroChem* **2** 1479–86
- [131] Miller D J, Proff C, Wen J G, Abraham D P and Bareño J 2013 Observation of Microstructural Evolution in Li Battery Cathode Oxide Particles by In Situ Electron Microscopy *Adv. Energy Mater.* **3** 1098–103